Int. J. Heat Mass Transfer. Vol. 26, No. 3, pp. 459–464, 1983
Printed in Great Britain

0017-9310/83/030459-06 $03.00/0
Pergamon Press Ltd.

POST-DRYOUT HEAT TRANSFER IN STEAM GENERATOR TUBES AT HIGH PRESSURES

H. C. ÜNAL and M. L. G. VAN GASSELT
Division of Technology for Society—TNO, P.O. Box 342, 7300 AH Apeldoorn, The Netherlands

(*Received* 5 *February* 1982)

Abstract—Post-dryout heat transfer coefficients were determined in a 10 m long sodium (i.e. non-uniformly) heated steam generator tube of 7.86 mm I.D. for the pressure range from 14.8 to 19.9 MN m^{-2}. The present data and data from the literature obtained from electrically (i.e. uniformly) heated tubes were correlated using dimensional analysis. The ranges of geometries and operating conditions of these data are: Tube length: 0.61–10 m; tube diameter: 2.54–20 mm; pressure: 14.8–19.9 MN m^{-2}; mass velocity: 415–3500 kg m^{-2} s^{-1}; heat flux: 5.3–166.2 W cm^{-2}; thermodynamic steam quality: 0.21–1. The number of data considered is 639. The correlation presented predicts the post-dryout heat transfer coefficient from these data within 20% accuracy for 95% of the time. The RMS error for all the data is 10.85%.

NOMENCLATURE

- b, Laplace constant [m];
- d, tube inside diameter [m];
- G, mass velocity [kg m^{-2} s^{-1}];
- g, acceleration of gravity [m s^{-2}];
- H_l, enthalpy of water at the state of saturation [J kg^{-1}];
- h, post-dryout heat transfer coefficient [W m^{-2} K^{-1}];
- k, thermal conductivity of steam [W m^{-1} K^{-1}];
- L, tube length [m];
- Nu, Nusselt number;
- n, number of data;
- P, pressure [N m^{-2}];
- Pr, Prandtl number;
- P_r, reduced pressure, P/P_c;
- q, heat flux [W m^{-2}];
- t, temperature [°C];
- t_{sat}, saturation temperature [°C];
- X, thermodynamic steam quality.

Greek symbols

- ζ, axial coordinate [m];
- ρ_l, density of water at the state of saturation [kg m^{-3}];
- ρ_v, density of steam at the state of saturation [kg m^{-3}];
- μ, dynamic viscosity of steam [kg m^{-1} s^{-1}];
- σ, surface tension [N m^{-1}].

Subscripts

- c, refers to value at the critical point;
- f, refers to film temperature;
- M, refers to measured value;
- P, refers to predicted value;
- w, refers to wall condition.

INTRODUCTION

THIS study deals with post-dryout heat transfer in non-uniformly and uniformly heated vertically orientated circular steam generator tubes for the pressure range of $14.8 \leqslant P$ (MN m^{-2}) $\leqslant 19.9$. Post-dryout heat transfer data and correlations for this pressure range and for vertical steam generator tubes have been reported [1–6]. The data of refs. [1–3] have been obtained in electrically (i.e. uniformly) heated tubes. To the knowledge of the authors, no post-dryout heat transfer data are available in the literature from non-uniformly heated tubes and for the pressure range considered in this study. The correlations given in refs. [1, 2, 4–6] are of an empirical nature, and are modifications of the Dittus–Boelter equation. For the correlation of data, the effect of thermal non-equilibrium in the post-dryout region on heat transfer has been considered [6]. The resulting correlation is, however, too complex for practical calculations. As a general rule, an empirical post-dryout heat transfer correlation is only applicable to the range of data from which it is derived [6].

In the post-dryout region of a steam generator tube, thermal non-equilibrium exists between the phases, as liquid droplets at the saturation temperature are present in the superheated steam. Consequently the true steam quality in this region is lower than the thermodynamic steam quality and the temperature of steam is higher than the saturation temperature. Analytical models have been given in the literature to determine post-dryout heat transfer [7–11]. In these models, a dispersed droplet flow regime has been assumed. In most models, heat transfer to the vapour from the heated surface and heat transfer to the liquid droplets from the vapour have been considered but heat transfer to the liquid droplets from the heated wall has been neglected. Heat transfer to the vapour from the heated wall has always been calculated using a correlation for single phase flow. The model of ref. [7] has been verified with nitrogen data, the model of ref. [8] with refrigerant data, the models of refs. [9, 10] with water data taken at pressures lower than 12 MN m^{-2} and the model of ref. [11] with water data obtained at $P = 6.9$ MN m^{-2} and with nitrogen data. Each of these models appeared to give satisfactory results. No analytical model has been tested with water data obtained at pressures higher than 12 MN m^{-2}. For the

preparation of an analytical model, empirical data are required, among other things, for the motion and the diameters of the liquid droplets. Such data are scarce in the literature [11], and are not yet available for the flow of water–steam mixtures at high pressures.

In ref. [12], data for temperature oscillations in the post-dryout region are reported for water. These oscillations have been measured in the present test tube and in an 18.84 m long tube of 7.86 mm I.D. with a 0.5 mm O.D. thermocouple located in the cross-section of each tube 2.34 mm from the heated wall for $P = 6.2$–$18.2\ \mathrm{MN\ m^{-2}}$ and $X = 1.02$–1.51. Both test tubes were heated by sodium. The water droplets at saturation temperature present in the superheated steam should irregularly wet the tip of the thermocouple. The amount of the water droplets in any part of the cross-section of the tube can be assumed to vary randomly. Consequently the tip of the thermocouple would be heated up and cooled down irregularly. The maximum peak-to-peak amplitudes of the oscillations observed varied from 4 to 25 K and decreased with increasing pressure and outlet temperature. Their periods were small. They completely faded away at $P = 20\ \mathrm{MN\ m^{-2}}$. The foregoing probably implies that the thermal non-equilibrium between the phases in the post-dryout region of a steam generator tube is not of considerable significance for high pressures. It is also reported [6] that for the evaluation of temperature and heat transfer coefficient in the post-dryout region, the assumption of thermal equilibrium between the phases yielded satisfactory results in most cases for water at high pressures (i.e. $P > 17\ \mathrm{MN\ m^{-2}}$).

A review of the work on the post-dryout heat transfer carried out till the mid-1970s is given in ref. [13]. Recent work on the subject has been reviewed [10, 11].

The aim of this study is the presentation of data for the post-dryout heat transfer coefficient obtained from a sodium (i.e. non-uniformly) heated steam generator tube of 7.86 mm I.D. for $P = 14.8$–$19.9\ \mathrm{MN\ m^{-2}}$ and $G = 415$–$3467\ \mathrm{kg\ m^{-2}\ s^{-1}}$. These data and the data of refs. [2, 3] obtained from electrically (i.e. uniformly) heated tubes for $d = 2.54$–20 mm, $P = 16.6$–$19.5\ \mathrm{MN\ m^{-2}}$ and $G = 700$–$3500\ \mathrm{kg\ m^{-2}\ s^{-1}}$ have been correlated using dimensional analysis.

EXPERIMENTAL APPARATUS, PROCEDURE AND DATA REDUCTION

A 10 m long test tube of 7.86 mm I.D. and 12 mm O.D. was used. This tube was manufactured from stainless steel, grade AISI-316. The sodium side surrounding the test tube was constructed in the form of seven annuli, as shown in Fig. 1. Counting from the base, the first three annuli were 1.977 m long and the last four annuli were 0.989 m long. The distance between the successive annuli was 16 mm. The inner wall of each annulus was formed by the test tube. The I.D. of the outer tube of each annulus was 25 mm. The annuli were connected by approximately 0.5 m long adiabatic circular tubes of 25 mm I.D. The flow orientation was upward on the water–steam side and downward on the sodium side. This test tube was installed in a heat transfer loop, which is described elsewhere [12, 14].

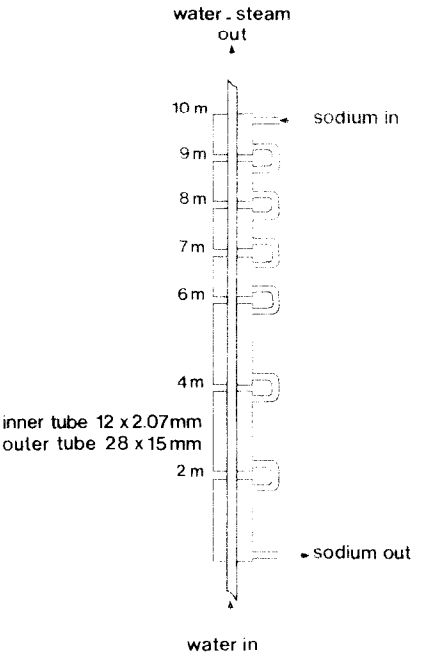

FIG. 1. Construction of the test tube.

The test tube was heavily instrumented. It is considered sufficient to mention here that both on the sodium side and on the water–steam side, outlet pressure, mass flow and temperature at $\zeta = 0$ (i.e. at the inlet of the test tube), 2, 4, 6, 7, 8, 9 and 10 m (i.e. at the outlet of the test tube) were measured. In the last 4 m part of the tube, wall temperatures were also measured at 34 axial positions at a nominal radius of 4.68 mm.

All the measurements were carried out with pre-calibrated instruments, collected with an on-line data acquisition system, and processed by a Hewlett-Packard 2116-B computer. This computer had a 32 kbytes core memory and 1000 kbytes auxiliary disc memory for data storage.

Both the sodium side and water steam side mass flows were measured with turbine flow meters, which had errors less than 1%. For measuring the water–steam side outlet pressure, a dead-weight balance manometer was used, which had a maximum error of 30 $\mathrm{kN\ m^{-2}}$. Both on the sodium side and on the water–steam side, temperatures were measured with chromel–alumel thermocouples of 0.5 mm O.D. For measuring the wall temperatures, chromel–alumel thermocouples of 0.34 mm O.D. were used. The maximum error in measuring the above mentioned temperatures was 1.2 K. The wall thermocouples were calibrated using two procedures. First their readings were corrected in accordance with the readings of the pre-calibrated water–steam- and sodium-side thermocouples during isothermal runs. Secondly, the exact location of each wall thermocouple was determined. For this purpose, a great number of single-phase forced convection runs were made. Assuming that the sodium-side tempera-

ture is linear between the locations of two successive thermocouples and that the sodium-side heat transfer coefficient is given by the modified Lyon equation [15], the location of each wall thermocouple was determined using Fourier's law of conduction. Thereafter, for each meter-section of the test tube, the average heat flux calculated by using the values of local heat fluxes determined with the aid of the wall thermocouples was compared with the heat flux calculated by using a heat balance. These two average heat fluxes differed by less than 6%. This accuracy seems to be acceptable at the present state of the art, as will be explained when correlating the data.

Demineralised water with an oxygen content of less than 15 ppb, a conductivity of less than 0.5 μS cm^{-1} and a pH between 8.5 and 9 was used during the tests.

Before each test run, steady-state conditions were established. These conditions were assumed to have been reached, when the variation in the sodium-side inlet temperature, the water–steam side inlet temperature, the sodium-side mass flow and the water–steam side mass flow had not exceeded 0.5 K min^{-1}, 0.5 K min^{-1}, 0.3% and 0.1%, respectively. The variation of the water–steam side pressure stayed within 30 kN m^{-2}.

All the measurements made were first transformed into a graphical form on the computer by plotting, among other things, local heat flux, sodium-side and water–steam-side bulk and wall temperatures, water–steam-side heat transfer coefficient and steam quality versus the length of the test tube. Smooth curves were drawn through the measured or calculated values. The local heat flux, post-dryout heat transfer coefficient and steam quality were then evaluated from these smooth curves. A typical plot of measurements is given in ref. [14].

The properties of water, steam and sodium were evaluated from the data given in the tables of ref. [16] and the formulas of ref. [17]. For the evaluation of the value of a property from the data given in a table of ref. [16], the values of this property for appropriate ranges of temperature and pressure were fitted in a high-degree polynomial.

In total, 744 data were obtained [18]. 468 data which were taken at film temperatures equal or higher than 370°C were considered for further analysis. This was for the elimination of the probable errors for the evaluation of the properties of steam. These properties and especially the Prandtl number of steam vary drastically at high pressures and in the vicinity of the saturation temperature. The range of operating conditions for these 468 data are summarized in Table 1.

CORRELATION OF DATA

Before an attempt was made to correlate the data, they were first compared with the correlations of Miropol'skiy [1], Kon'kov and Zuperman [4], and Herkenrath *et al.* [5]. These correlations predict the post-dryout heat transfer coefficient from the data within deviation of −16 and 202%, −25 and 185% and −21 and 112%, respectively. The RMS errors reported are 69.1, 57.8 and 48.9%. The span of deviation of these correlations in fitting the data is probably due to the fact that they have been derived from the data obtained in electrically (i.e. uniformly) heated tubes.

For the correlation of the present data and the 133 data of ref. [3] taken in electrically heated tubes of 10 and 20 mm I.D. for $17 \leqslant P[\mathrm{MN\ m^{-2}}] \leqslant 19.5$ and $700 \leqslant G[\mathrm{kg\ m^{-2}\ s^{-1}}] \leqslant 3500$, dimensionless analysis was applied. The ranges of geometries and operating conditions of the 133 data of ref. [3] considered in the present study are given in Table 1. These 133 data were randomly selected from the graphs of ref. [3].

The correlation obtained is

$$Nu_f = 0.0091 a_1 a_2 a_3 a_4 a_5 a_6 a_7 a_8, \tag{1}$$

$$Nu_f = hd/k_f, \tag{2}$$

$$h = q/(t_w - t_{sat}), \tag{3}$$

$$a_1 = \left\{\frac{Gd}{\mu_f}[X + (1-X)\rho_v/\rho_l]\right\}^{1.154}, \tag{4}$$

$$a_2 = Pr_f^{0.577}, \tag{5}$$

$$a_3 = (k_f/k_c)^{0.595}, \tag{6}$$

$$a_4 = (t_f/t_c)^{-2.17}, \tag{7}$$

$$a_5 = P_r^{0.212}(1-P_r)^{-0.27}, \tag{8}$$

$$a_6 = [G^2/(\rho_l^2 dg)]^{0.0396}, \tag{9}$$

$$a_7 = [q/(H_l G)]^{0.44}, \tag{10}$$

$$a_8 = 1. \tag{11}$$

Table 1. Ranges of geometries and operating conditions for the present data and the data of ref. [3]

	Present data			Data of Herkenrath *et al.* [3]			
Geometry	$d = 7.86$ mm; $L = 10$m			$d = 10$ mm; $L = 5.1$ m			$d = 20$ mm $L = 8.5$ m
P (MN m^{-2})	14.81–16.50	16.51–18.00	18.01–19.90	17.0	18.5	19.5	18.5
G (kg m^{-2} s^{-1})	824–1667	569–3467	415–1748	700–3500	700–3500	700–3500	700–3500
q (W cm^{-2})	14.5–66.6	8.1–121.0	5.3–59.1	30–140	30–160	30–160	30–140
X	0.44–0.98	0.33–1.00	0.37–1.00	0.34–1.00	0.26–1	0.21–0.89	0.27–0.67
Nu_M	200–867	166–2170	149–1390	201–3842	204–2974	195–2392	413–5947
T_f (°C)	370–375.8	370–382.9	372–378.4	370–457	380–454	385–462	381–460
n	32	271	165	37	40	32	24

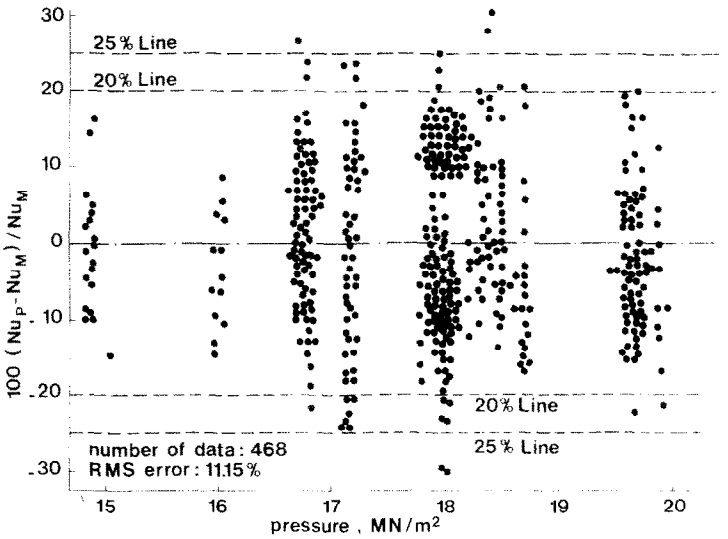

FIG. 2. Errors in predicting the heat transfer coefficient from the present data.

The dimensionless numbers in equations (2), (4) and (5) are common to all empirical post-dryout heat transfer correlations and, therefore, they are not explained here.

As stated before, at high pressures and in the vicinity of the saturation temperature, the thermal conductivity, viscosity and in particular the Prandtl number of steam changes drastically. This is the reason why the dimensionless numbers given in equations (6)–(8), i.e. reduced-thermal conductivity, -temperature and -pressure, were used to compensate for the effect of variation of the properties of steam especially with changing pressure and temperature on the post-dryout heat transfer coefficient. For instance, for the present tests, the film temperatures varied between 370 and 382.9°C, while for the tests of ref. [3] considered in this study, a variation between 370 and 462°C was observed (Table 1). This implies that the term expressed by equation (7) varies between 1.02 and 0.95 for the present data and between 1.02 and 0.63 for the data of ref. [3]. This means that the present data could be correlated well without considering a_4 in equation (1) (i.e. accurate to 25% for 99.6% of the time). However, in this case, it failed to properly correlate the data of ref. [3].

The Froude number in equation (9) shows the ratio of inertia to gravity force, and was considered to take into account the settling of liquid droplets in the vapour [19].

The modified boiling number in equation [10] takes into account the non-uniformity of the axial heat flux distribution. For a non-uniformly heated steam generator tube (say, the present test tube), this boiling number changes along the length of the tube if the pressure in the tube is assumed constant. For an electrically (i.e. uniformly) heated tube, this boiling number is constant along the tube if a constant pressure is considered in the tube. It is logical to assume that the increase of heat flux along the post-dryout region will quicken droplet evaporation; consequently, the heat transfer mechanism in this region will be affected.

The results of comparing the data with equation (1) are shown in Figs. 2 and 3. This equation predicts the Nusselt number, and consequently the post-dryout heat transfer coefficient, within 20% accuracy for 94% of the time from the present data and within 20% accuracy for 97% of the time from the data of ref [3]. The RMS error is 11.15% for the present data and 9.82% for the data of [3].

Equation (1) was also compared with the data of [2] taken in small-diameter short vertical tubes of 2.54 and

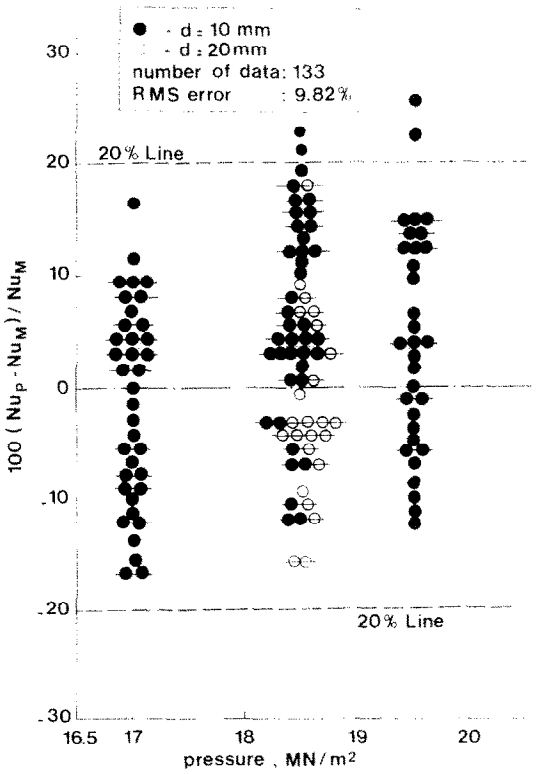

FIG. 3. Errors in predicting the heat transfer coefficient from the data of ref. [3].

Table 2. Ranges of geometries and operating conditions for the data* of ref. [2]

L (m)	0.61, 1.83 and 2.75			
d (mm)	2.54		5.08	
P (MN m^{-2})	16.6–16.8	19.5	16.8	19.4
G (kg m^{-2} s^{-1})	2034–2712	2034–2712	2034–3376	2034
q(W cm^{-2})	129.6–149.2	134.3–166.2	91.3–152.6	90.7
X	0.30–0.66	0.34–0.77	0.37–0.96	0.54–0.90
Nu_M	166–345	212–620	559–1660	729–1297
T_f (°C)	413–467	395–451	371–416	378–393
n	9	8	17	4

* Data obtained in the stable region after the critical heat flux.

5.08 mm I.D. for $16.6 \leqslant P$ (MN m^{-2}) $\leqslant 19.5$. The ranges of geometries and operating conditions of these data are summarized in Table 2. The data obtained in tubes of 2.54 mm I.D. at $P = 16.6$–16.8 MN m^{-2} did not fit equation (1) well, i.e. within deviation of -33 and -51%. The remaining data, however, fitted the correlation fairly well, i.e. within deviation of 4 and -22% with a RMS error of 11.67%. Bergles and Rohsenow [20] report that the single-phase forced convection heat transfer coefficient in a small-diameter tube of 2.39 mm I.D. is about 10% higher than that predicted by the Dittus–Boelter correlation. The foregoing implies that the effect of a small tube diameter on post-dryout heat transfer is of significance, and this effect is probably due to the turbulence created by the liquid droplets.

In order to properly correlate the data of ref. [2] taken in small-diameter tubes, equation (1) was slightly modified, i.e. the expression given by equation (11) was transformed into the following form:

$$a_8 = 1 + 138.5(b/d)^{5.02} \tag{12}$$

where b, the Laplace constant, is

$$b = \{\sigma/[g(\rho_l - \rho_v)]\}^{0.5}. \tag{13}$$

In this case, equation (1) predicts the post-dryout heat transfer coefficient from the data of ref. [2] within 18% accuracy for 97% of the time with a RMS error of 10.57%. a_8 given by equation (12) is equal to practically 1 for the conditions of the present data and of the data of ref. [3].

The above mentioned deviations are considered to be quite satisfactory taking into account that the scatter on post-dryout heat transfer coefficients determined in four identical test sections by four different groups of investigators was between 10 and 25% with a mean of 17.9% [13].

The ranges of geometries and operating conditions of the data used to establish equation (1) are recapitulated below: Geometry: sodium and electrically heated and vertically orientated circular tubes; $L = 0.61$–10 m; $d = 2.54$–20 mm; $P = 14.8$–19.9 MN m^{-2}; $G = 415$–3500 kg m^{-2} s^{-1}; $X = 0.21$–1.00; $q = 5.3$–166.2 W cm^{-2}. The number of data considered is 639. The correlation presented predicts the post dryout heat transfer coefficient from these data within 20% accuracy for 95% of the time. The RMS error for all the data is 10.85%.

Acknowledgements—This study is a government sponsored work carried out by TNO. The authors wish to express their gratitude to K. A. Warschauer for his encouragements and comments. P. J. de Munk has carried out the experiments. A. D. Koppenol and G. Wentink assisted in the evaluation and correlation of the data.

REFERENCES

1. Z. L. Miropol'skiy, Heat transfer in film boiling of a steam–water mixture in steam generating tubes, *Teploenergetika* **10**(5), 49–52 (1963).
2. A. A. Bishop, R. O. Sandberg and L. S. Tong, Forced convection heat transfer at high pressure after the critical heat flux, ASME paper-65-HT-31 (1965).
3. H. Herkenrath, P. Mörk-Mörkenstein, U. Jung and F. J. Weckermann, Wärmeübergang an Wasser bei erzwungener Ströming im Druckbereich von 140 bis 250 Bar, Euratom report, EUR 3658 d (1968).
4. A. S. Kon'kov and D. A. Zuperman, Experimental study of heat transfer to wet steam, *Teploenergetika* **14**(3), 54–56 (1967).
5. H. Herkenrath and P. Mörk-Mörkenstein, Die Wärmeübergangkrise von Wasser bei erzwungener Ströming unter hohen Drücken, *Atomkernenergie* **14**(6), 403–407 (1969).
6. D. C. Groeneveld and G. G. J. Delorme, Prediction of thermal non-equilibrium in the post-dryout regime, *Nucl. Engng Des.* **36**, 17–26 (1976).
7. R. P. Forslund and W. M. Rohsenow, Thermal non-equilibrium in dispersed flow film boiling in a vertical tube, MIT report-75312-44 (1966).
8. Y. Koizumi, T. Ueda and H. Tanaka, Post dryout heat transfer to R-113 upward flow in a vertical tube, *Int. J. Heat Mass Transfer* **22**, 669–678 (1979).
9. A. W. Bennett, G. F. Hewitt, H. A. Kearsey and R. K. F. Keeys, Heat transfer to steam–water mixtures flowing in uniformly heated tubes in which the critical heat flux has been exceeded, AERE-R5373 (1967).
10. P. Saha, A nonequilibrium heat transfer for dispersed droplet post-dryout regime, *Int. J. Heat Mass Transfer* **23**, 483–492 (1980).
11. C. F. Delale, Lower bound estimate for droplet size in two-phase dispersed flow, *J. Heat Transfer* **102**, 501–507 (1980).
12. H. C. Ünal, An investigation of the inception conditions of dynamic instabilities in sodium heated steam generator pipes, in *Two-Phase Flows and Heat Transfer* (edited by S. Kakaç and T. N. Veziroglu) Vol. 3, pp. 1425–1443. Hemisphere, Washington (1977).

13. J. G. Collier, Post-dryout heat transfer—A review of the current position, in *Two-Phase Flows and Heat Transfer* (edited by S. Kakaç and T. N. Veziroglu) Vol. 2, pp. 769–813. Hemisphere, Washington (1977).
14. P. J. de Munk, Two-phase flow experiments in a 10 m long sodium heated steam generator test section, *Proc. Int. Meeting on Reactor Heat Transfer*, Karlsruhe, 9–11 October, pp. 504–518 (1973).
15. Liquid Metals Handbook—Sodium-NaK Supplement, p. 77. Atomic Energy Commission, Department of the Navy, Washington D.C., U.S.A. (1955).
16. E. Schmidt, *Properties of Water and Steam in SI-Units*, Springer, Berlin (1969).
17. M. E. Durham, The thermodynamic and transport properties of liquid sodium, CEGB-Report-RD/B/M2479 (Revised)-CFR/THWP/P(72) 28 (1974).
18. P. J. de Munk, A. D. Koppenol and B. J. Stam, Warmte-overdracht- en drukvalmetingen in een natriumverhitte stoomgenerator testsectie in het drukbereik van 150 tot 200 bar, een compilatie van metingen, TNO-Report, Report No. 74-0839 (1974) (Confidential).
19. J. G. Knudsen and D. L. Katz, *Fluid Dynamics and Heat Transfer*, p. 137. McGraw-Hill, New York (1958).
20. A. E. Bergles and W. M. Rohsenow, The determination of forced-convection surface boiling heat transfer, *J. Heat Transfer* **86**, 365–372 (1964).

TRANSFERT THERMIQUE APRES L'ASSECHEMENT DANS DES TUBES DE GENERATEUR DE VAPEUR A GRANDE PRESSION

Résumé—Des coefficients de transfert thermique après l'assèchement sont déterminés dans un tube de 10 m chauffé au sodium de 7,86 mm de diamètre intérieur, pour des pressions allant de 14,8 à 19,9 MN m^{-2}. Les résultats obtenus et les données de la littérature obtenus pour des tubes chauffés électriquement (uniformément) sont rassemblés en utilisant l'analyse dimensionnelle. Les domaines des géométries et des conditions opératoires de ces essais sont : longueur du tube : 0,61–10 m ; diamètre du tube : 2,54–20 mm ; pression : 14,8–19,9 MN m^{-2} ; vitesse massique : 415–3500 kg m^{-2} s^{-1} ; flux thermique : 5,3–166,2 W cm^{-2} ; qualité thermodynamique de la vapeur : 0,21–1. Le nombre de données est 639. La formule présentée donne le coefficient de transfert après assèchement à 20% près pour 95% des points. L'erreur quadratique moyenne pour toutes les données est 10,85%.

POST-DRYOUT-WÄRMEÜBERTRAGUNG IN DAMPFERZEUGERROHREN BEI HOHEN DRUCKEN

Zusammenfassung—Post-dryout-Wärmeübertragungskoeffizienten wurden in einem 10 m langen, von Natrium (d.h. ungleichförmig) beheizten Dampferzeugerrohr mit 7,86 mm Innendurchmesser für einen Druckbereich von 14,8 bis 19,9 MN m^{-2} bestimmt. Mittels Dimensionsanalyse wurden die erhaltenen Daten sowie Literaturwerte, die mit elektrisch (d.h. gleichmäßig) beheizten Rohren bestimmt wurden, korreliert. Die Bereiche der geometrischen Werte und der Versuchsbedingungen waren folgende: Rohrlänge: 0,61 ÷ 10 m; Rohrdurchmesser: 2,54 ÷ 20 mm, Druck: 14,8 ÷ 19,9 MN/m^2; Massenstromdichte: 415 ÷ 3500 kg m^{-2} s^{-1}; Wärmestromdichte: 5,3 ÷ 166,2 W m^{-2}; thermodynamischer Dampfgehalt: 0,21 ÷ 1,0. Es wurden 639 Meßpunkte berücksichtigt. Die vorgeschlagene Beziehung ermöglicht die Berechnung des Post-dryout-Wärmeübergangskoeffizienten, der sich aus diesen Daten ergibt, mit einer Genauigkeit von 20%. Der mittlere quadratische Fehler aller Daten liegt bei 10,85%.

ЗАКРИТИЧЕСКИЙ ТЕПЛОПЕРЕНОС В ТРУБАХ ПАРОГЕНЕРАТОРОВ ПРИ ВЫСОКИХ ДАВЛЕНИЯХ

Аннотация—Определены коэффициенты закритического теплопереноса в неоднородно нагреваемой натрием трубе парогенератора, имеющей длину 10 м и внутренний диаметр 7,86 мм, в диапазоне давлений от 14,8 до 19,9 Мн/м^2. С помощью анализа размерностей проведено сопоставление полученных результатов с опубликованными данными для электрически (т.е. однородно) нагреваемых труб. Эти данные были получены для следующих геометрий и рабочих параметров: длина трубы 0,61–10 м, диаметр трубы 2,54–20 мм, давление 14,8–19,9 Мн/м^2, массовая скорость 415–3500 кг/м^{2}сек, тепловой поток 5,3–166,2 Вт/см^2, термодинамическое весовое паросодержание 0,21–1. Рассмотрено 639 значений. С помощью предложенного обобщенного соотношения по этим данным можно рассчитать коэффициент закритического теплопереноса с точностью до 20% для 95% времени. Среднеквадратичная погрешность во всех случаях не превышает 10,85%.